Crystal structure of carboxylesterase from *Pseudomonas fluorescens*, an α/β hydrolase with broad substrate specificity

Kyeong Kyu Kim[1], Hyun Kyu Song[1], Dong Hae Shin[1], Kwang Yeon Hwang[1], Senyon Choe[2], Ook Joon Yoo[3] and Se Won Suh[1]*

Background: A group of esterases, classified as carboxylesterases, hydrolyze carboxylic ester bonds with relatively broad substrate specificity and are useful for stereospecific synthesis and hydrolysis of esters. One such carboxylesterase from *Pseudomonas fluorescens* is a homodimeric enzyme, consisting of 218-residue subunits. It shows a limited sequence similarity to some members of the α/β hydrolase superfamily. Although crystal structures of a number of serine esterases and lipases have been reported, structural information on carboxylesterases is very limited. This study was undertaken in order to provide such information and to understand a structural basis for the substrate specificity of this carboxylesterase.

Results: In this study, the crystal structure of carboxylesterase from *P. fluorescens* has been determined by the isomorphous replacement method and refined to 1.8 Å resolution. Each subunit consists of a central seven-stranded β sheet flanked by six α helices. The structure reveals the catalytic triad as Ser114–His199–Asp168. The structure of the enzyme in complex with the inhibitor phenylmethylsulfonyl fluoride has also been determined and refined to 2.5 Å. The inhibitor is covalently attached to Ser114 of both subunits, with the aromatic ring occupying a hydrophobic site defined by the aliphatic sidechains of Leu23, Ile58, Ile70, Met73 and Val170. No large structural changes are observed between the free and inhibitor-bound structures.

Conclusions: Carboxylesterase from *P. fluorescens* has the α/β hydrolase fold and the Ser–His–Asp catalytic triad. The active-site cleft in each subunit is formed by the six loops covering the catalytic serine residue. Three of the active-site loops in each subunit are involved in a head-to-head subunit interaction to form a dimer; it may be these extra structural elements, not seen in other esterases, that account for the inability of carboxylesterase to hydrolyze long chain fatty acids. As a result of dimerization, the active-site clefts from the two subunits merge to form holes in the dimer. The active-site clefts are relatively open and thus the catalytic residues are exposed to the solvent. An oxyanion hole, formed by nitrogen atoms of Leu23 and Gln115, is present in both the free and inhibitor-bound structures. An open active site, as well as a large binding pocket for the acid part of substrates, in *P. fluorescens* carboxylesterase may contribute to its relatively broad substrate specificity.

Addresses: [1]Department of Chemistry, College of Natural Sciences, Seoul National University, Seoul 151-742, Korea, [2]Structural Biology Laboratory, Salk Institute, La Jolla, CA 92037, USA and [3]Department of Biological Sciences, Korea Advanced Institute of Science and Technology, Taejon 305-701, Korea.

*Corresponding author.
E-mail: sewonsuh@plaza.snu.ac.kr

Key words: α/β hydrolase, carboxylesterase, *Pseudomonas fluorescens*, substrate specificity

Received: **11 August 1997**
Revisions requested: **29 August 1997**
Revisions received: **29 September 1997**
Accepted: **8 October 1997**

Structure 15 December 1997, **5**:1571–1584
http://biomednet.com/elecref/0969212600501571

Introduction

Many man-made chemicals including drugs and pesticides are ester compounds. Their hydrolysis is catalyzed by esterases, a class of ubiquitous enzymes. Esterases are distinguished from their close relatives, lipases, by the lack of interfacial activation. One group of esterases, classified as carboxylesterases or carboxylic-ester hydrolases (EC 3.1.1.1), catalyze the hydrolysis of short-chain aliphatic and aromatic esters with broad substrate specificity and are inhibited by organophosphates [1]. Carboxylesterases play an important part in the detoxification of organophosphorous compounds in mammalian systems [2]. Microbial carboxylesterases have been utilized in the synthesis of ester compounds in non-aqueous solvents and also in stereospecific hydrolysis, due to their broad substrate specificity and high stereoselectivity [3,4]. In the presence of alcohol, a heat-stable carboxylesterase catalyzes the transfer of the substrate acyl group to alcohol groups [5]. A novel carboxylesterase identified in *Rhodococcus* sp. H1 was able to hydrolyze heroin into morphine and is being

developed as one of the components for a heroin biosensor [6]. In the human liver, carboxylesterase plays an important role in drug metabolism [7].

The amino acid sequence data on carboxylesterases indicate that they belong to the superfamily of α/β hydrolase fold enzymes. Despite their important biological functions, no studies have been made on the three-dimensional structure of any carboxylesterase. A wealth of structural information on a number of serine hydrolases, belonging to the α/β hydrolase superfamily, however, is available. The serine hydrolases have a core structure composed of a central, predominantly parallel, β-pleated sheet surrounded by α helices [8], and their catalytic machinery is typically composed of Ser–His–Asp/Glu. The available structural data include many crystal structures of lipases, a special class of α/β hydrolases [9–17]. In their closed conformation, the lipase active site is buried underneath a short helical segment, called a 'lid' (or a 'flap'). The opening of this lid is believed to be one of the key elements of interfacial activation in lipases, because cutinase, a lipolytic enzyme showing no interfacial activation, has only a mini lid covering the active site [18–20]. Cutinase may be considered as a link between true esterases and true lipases. Furthermore, crystal structures of other α/β hydrolase fold enzymes, distantly or closely related to the carboxylesterases, have been reported: dienelactone hydrolase from *Pseudomonas* sp. B13 (DLH; [21]), haloalkane dehalogenase from *Xanthobacter autotrophicus* [22], acetylcholinesterase [23], cholesterol esterase [24], carboxypeptidase II from wheat [25] and thioesterase from *Vibrio harveyi* [26]. Many of these enzymes share similar or related catalytic reaction mechanisms; nevertheless, they exhibit widely different substrate specificities.

Carboxylesterase from *Pseudomonas fluorescens* is a homodimeric enzyme, with each subunit comprising 218 amino acid residues (subunit Mr 23,856). It is readily inhibited by serine hydrolase inhibitors such as phenylmethylsulfonyl fluoride (PMSF). This is consistent with the presence of the characteristic Gly–X–Ser–X–Gly sequence [27], which is conserved in the catalytic site of many serine hydrolases [28]. This carboxylesterase hydrolyzes methyl esters of short to medium chain (C2–C10) fatty acids and also hydrolyzes phenylacetate and *p*-nitrophenyl esters of short chain fatty acids [27]. It also hydrolyzes triacetin and tributyrin but shows little hydrolyzing activity against triglycerides of longer chain fatty acids. In contrast to the relatively broad specificity for the acid part of the substrate, its specificity toward the alcohol moiety of acetate esters is somewhat limited, being unable to hydrolyze ethyl, *n*-propyl, *n*-butyl or α-naphthyl acetates [27]. It therefore will be interesting to compare the structures of different α/β hydrolase fold enzymes in order to understand a structural basis for the difference in substrate specificities. Here, we report the crystal structure of the uninhibited carboxylesterase from *P. fluorescens* determined by the multiple isomorphous replacement as well as that of the enzyme in complex with the inhibitor PMSF. Each subunit of the enzyme has the α/β hydrolase fold and the Ser–His–Asp catalytic triad; the two subunits interact in a head-to-head fashion to form a dimer. When the enzyme is inhibited by PMSF, Ser114 of both subunits is covalently modified but no large changes in the overall structure occur.

Results and discussion

Model quality and comparison of two subunits

The structure of the free (uninhibited) carboxylesterase has been determined by multiple isomorphous replacement method using nine heavy-atom derivatives (Table 1) and refined to 1.8 Å resolution. Each asymmetric unit of the crystal contains a homodimer. The refined model of the uninhibited enzyme comprises two subunits, each with all 218 residues as well as 247 water molecules. Subsequently, the structure of the enzyme inhibited by PMSF was also determined, and it was refined to 2.5 Å. Table 2 summarizes the refinement statistics, as well as model quality parameters for both models in the uninhibited and inhibited states. The average B factor for one subunit in the asymmetric unit is substantially higher than that for the other subunit (Table 2). This arises from the different extent of the two subunits involved in the crystal packing. For both the native and inhibited structures, only one non-glycine residue in each subunit is outside the allowed region in the Ramachandran plot — the catalytic residue Ser114 ($\phi = 62°, \Psi = -124°$ for one subunit and $\phi = 48°$, $\Psi = -112°$ for the other subunit of the uninhibited structure). It is, however, well defined by the electron density and its mean B factor is lower than the average value for each subunit: 17.4 Å^2 and 32.8 Å^2 for Ser114 and Ser614, respectively, of the uninhibited structure. (The sequence number of the second subunit starts from 501 to distinguish the two subunits.) This unique conformation around the catalytic serine has been observed in other α/β hydrolases [8] and has been termed a nucleophile elbow. For the sake of brevity, the subunit with a lower average B factor (subunit A) is mainly used in the following discussion, unless otherwise stated.

The non-crystallographic symmetry (NCS) between the two subunits of the dimer in the asymmetric unit of the crystal is a pseudo-twofold rotation of 175.8° without any translation. A superposition of non-crystallographically related subunits gives root mean square (rms) deviations of 0.40 Å and 0.84 Å for 873 mainchain and 809 sidechain atoms, respectively (for the inhibited enzyme, these values are 0.42 Å and 0.90 Å, respectively). In both the uninhibited and inhibited structures, only the segment between residues 73 and 77 shows rms deviations larger than 1.5 Å for the mainchain atoms.

Table 1

Data collection and phasing statistics.

Compound*	Soaking conc. (mM)	Soaking time (day)	No. of reflections	Resolution limit (Å)	Completeness (%)	R_{merge} † (%)	R_{iso} ‡ (%)	No. of sites	F_h/E§	R_{cullis} #
Native1 (SNU)			17,884	2.4	88.6	3.6				
Native2 (PF)			41,703	1.8	91.0	7.1				
PMSF-inhibited	100	3	15,245	2.5	88.5	4.3	15.6	2		
Pt	3.0	30	7143	3.2	81.6	3.7	16.4	2	0.67	0.86
Hg1	5.0	20	7888	3.2	90.1	4.0	22.1	4	0.67	0.86
Hg2	5.0	7	7703	3.2	88.0	4.9	27.6	6	1.04	0.73
Hg3	5.0	18	7260	3.2	90.6	4.0	34.2	3	1.12	0.72
Hg4	1.0	0.2	7822	3.2	89.3	4.8	25.0	5	0.94	0.78
Hg2 + Hg3	1.8 + 1.8	8	7761	3.2	88.7	3.6	20.1	4	0.84	0.78
Pt + Hg3	1.4 + 1.8	3	7747	3.2	88.5	3.3	19.9	5	0.83	0.78
Pt + Hg2 + Hg3	1.4 + 1.8 + 1.8	6	7637	3.2	87.2	3.3	16.1	9	1.29	0.65
Pt + Hg2 + Hg4	1.0 + 1.0 + 0.5	3	7850	3.2	89.6	3.8	15.0	7	0.99	0.74

*Pt = potassium platinum(II) cyanide; Hg1 = mercury bis(trifluoroacetate); Hg2 = 2-chloromercuri-4-nitrophenol; Hg3 = ethyl mercurithiosalicylic acid sodium salt; Hg4 = potassium mercury(II) iodide; SNU = Seoul National University; PF = Photon Factory.

†$R_{merge} = \Sigma|I_h - \langle I_h \rangle| / \Sigma I_h$. ‡$R_{iso} = \Sigma||F_{h,nat}| - |F_{h,der}|| / \Sigma|F_{h,nat}|$. §$F_h/E$, where F_h is the heavy atom structure factor and E is the residual lack of closure. #$R_{cullis} = \Sigma||F_{h,obs}| - |F_{h,calc}|| / \Sigma|F_{h,obs}|$.

Overall structure

The carboxylesterase subunit is globular with approximate dimensions of $40 \times 40 \times 35$ Å^3. The subunit structure consists of a seven-stranded, predominantly parallel, β sheet surrounded by six α helices (Figure 1). Figure 2 shows that the overall fold of carboxylesterase subunit is similar to the prototypic α/β hydrolase fold [8]. One major difference is that the first β strand (β1) of the prototypic α/β hydrolase

Table 2

Statistics for crystallographic refinement.

	Native	Inhibited
Resolution of data (Å)	8.0–1.8	8.0–2.5
Number of reflections with $F > 2\sigma_F$	40,600	15,125
R factor / R_{free}*(%)	20.8 / 27.3	18.1 / 25.4
Number of protein atoms excluding hydrogen	3364	3364
Number of heteroatoms / waters	– / 247	20 (2 PMSF) / 199
Root mean square deviations from ideal geometry		
Bond lengths (Å)	0.012	0.014
Bond angles (°)	1.23	1.38
Average B factors (Å^2)		
Mainchain atoms (A / B)†	20.9 / 35.9	21.0 / 33.5
Sidechain atoms (A / B)†	25.3 / 38.9	24.5 / 35.7
Waters	43.1	40.4
Heteroatoms	–	57.0 (PMSF)

*The R_{free} was calculated using 10% of the data. †A and B represent the subunits A (residues 1–218) and B (residues 501–718), respectively.

Figure 1

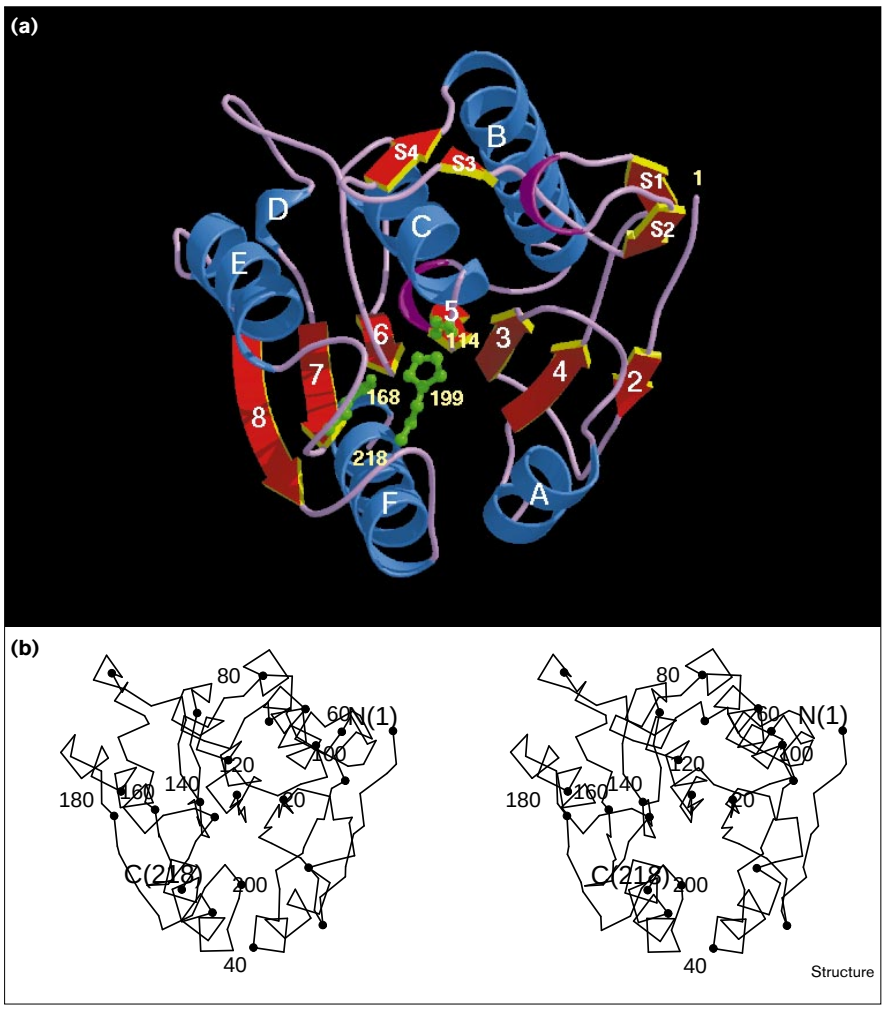

Subunit structure of *P. fluorescens* carboxylesterase, looking down the active site. **(a)** Ribbon diagram showing the secondary structure elements. Seven β strands (red arrows) are numbered sequentially from 2 to 8. Four short β strands (S1–S4) are also labeled. Six α helices (blue ribbons) are labeled sequentially from A to E. Two 3_{10} helices (G1 and G2, purple) are not labeled. The catalytic residues (Ser114, Asp168 and His199) are shown in green ball and stick representation **(b)** Stereo Cα trace. Every twentieth Cα atom is labeled.

fold is missing from this carboxylesterase subunit. To be consistent therefore with the nomenclature of Ollis *et al.* [8] and to facilitate comparisons with related structures, the first β strand in carboxylesterase is called β2. Among the seven strands in the central β sheet of carboxylesterase, six parallel β strands, β3–β8, provide the framework onto which the catalytic residues are placed (Figure 1). The remaining N-terminal strand β2, which is antiparallel to all the others, is not directly involved in the formation of the catalytic site. The first two β strands, β1 and β2, of the prototypic α/β hydrolase fold [8], therefore, appear to be dispensable for the catalytic activity. Further support for this suggestion is provided by the absence of these two β strands in the structures of cutinase from *Fusarium solani* [18] and lipases from *Pseudomonas glumae* [12] and *Pseudomonas cepacia* (PcL; [16,17]).

Catalytic triad, oxyanion hole and the active-site cleft

The catalytic triads of many α/β hydrolase fold enzymes have been observed to consist of Ser/Cys/Asp–His–Asp/Glu. The three-dimensional structure of *P. fluorescens* carboxylesterase reveals that its catalytic triad is formed by the three residues, Ser114–His199–Asp168, all located on the C-terminal side of the predominantly parallel β sheet (Figure 1). This is consistent with Ser114 being part of the characteristic Gly–X–Ser–X–Gly sequence; however, the two other catalytic residues could not have been predicted with confidence from the sequence information alone.

A comparison of the active-site features of this carboxylesterase with those of other α/β hydrolases leads us to suggest that an oxyanion hole is formed by nitrogen atoms of Leu23 and Gln115 in the uninhibited structure (Figure 3). The suggested oxyanion hole is similarly present in the inhibitor-bound structure (Figure 3). In this respect, *P. fluorescens* carboxylesterase is similar to cutinase which also has a preformed oxyanion hole [29]. In contrast to esterases, the oxyanion hole of lipases is absent in the inactive, closed, conformation and is formed only upon interfacial activation, which accompanies the opening of a helical

Figure 2

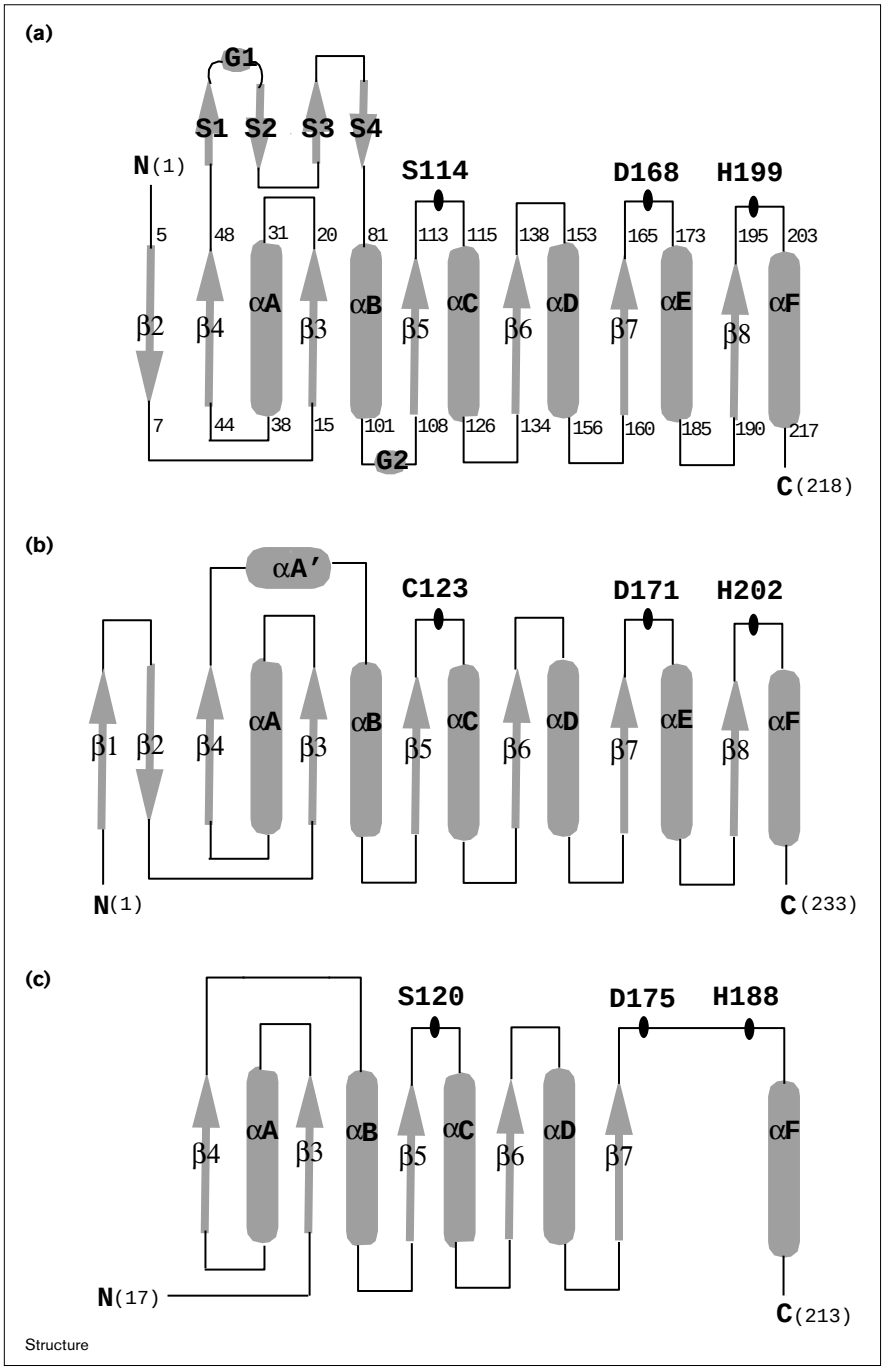

Topology diagram of **(a)** *P. fluorescens* carboxylesterase, **(b)** dienelactone hydrolase from *Pseudomonas* sp. B13 and **(c)** cutinase from *Fusarium solani*. Eight β strands (arrows) labeled as β1–β8 and six α helices (rods) labeled as αA–αF are possessed by the prototypic α/β hydrolase fold [8]. The catalytic residues are indicated by filled ovals. In (a), S1 (residues 53–55), S2 (63–65), S3 (70–72) and S4 (78–79) are the four short β strands, while G1 (residues 57–59) and G2 (105–107) are the two 3_{10} helices. The residue numbers at the N and C termini correspond to those in the crystal structures: three residues are missing from the C terminus of the dienelactone hydrolase model and a single residue is missing from each terminus of the cutinase model.

lid [30]. In the open conformation of PcL, the oxyanion hole is occupied by a water molecule [16]. No such water molecule is observed in this carboxylesterase structure.

Except for the sharply bent loop after β5 where the catalytic Ser114 is positioned, five other loops at the C-terminal ends of the parallel β strands are generally longer and have a more winding structure than those at the N-terminal ends of the parallel β strands (Figure 1). The six loops at the C-terminal ends of the parallel β strands form the active-site cleft in each subunit. The bottom of the cleft is formed by the three loops after strands β3, β5 and β6. A very winding loop structure after β4 forms a wall on one side of this cleft and two other loops after β7 and β8 form the other wall on the opposing side (Figure 1). The former, taller and thinner wall appears to be more flexible than the

Figure 3

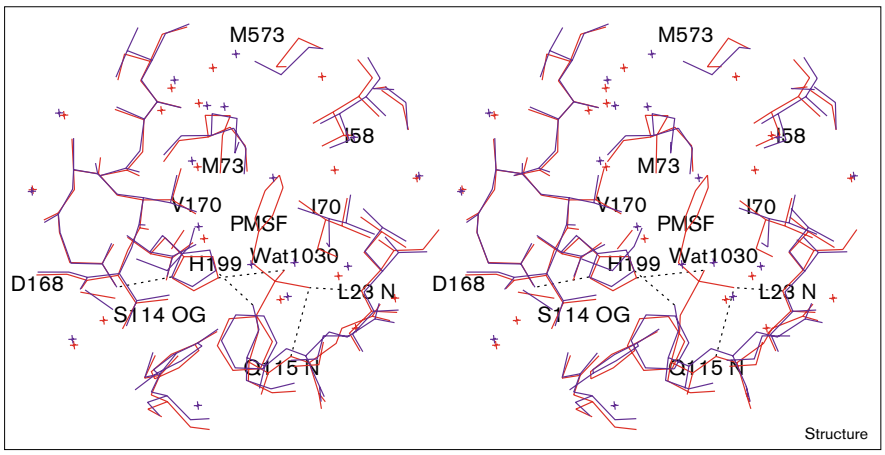

Stereo drawing of the active site of *P. fluorescens* carboxylesterase. The free and inhibitor-bound structures are colored in blue and red, respectively. The phenylmethylsulfonyl moiety of the inhibitor covalently bound to the Oγ atom of Ser114 is shown. The residues forming the catalytic triad and oxyanion hole, and also those surrounding the phenyl ring of the inhibitor, are labeled.

latter, on which the catalytic residues His199 and Asp168 are located with Asp168 positioned nearly at the top of the wall. The catalytic Ser114 is located deeply at the bottom of the active-site cleft near its center, with its sidechain being exposed to the solvent (Figures 4 and 5). One side of the active-site cleft is partially blocked by the sidechain atoms of Arg77, Tyr141 and Met175 (Figure 5). The two walls are involved in the dimerization and thus their inherent flexibility may be reduced. In the dimer, the two active-site clefts merge to form three small holes (Figure 4).

Inhibitor binding and structural changes

In order to obtain more detailed information about the structural alterations occurring during the catalysis, the structure of the enzyme in complex with the inhibitor PMSF has also been determined. When inhibited by PMSF, the enzyme is found to be covalently modified at the Oγ atom of Ser114. Both subunits in the dimer are observed to be modified (Figure 5). The two active sites in the dimer therefore must be separately available for the substrate. In the PMSF-inhibited structure, the sulfonyl group of the inhibitor makes hydrogen bonds with several residues: His199, Leu23 and Gln115 (Figure 3). A water molecule (Wat1030) in the uninhibited structure is displaced by one of the oxygen atoms in PMSF upon its binding (Figure 3). This water, present in both subunits of the free (uninhibited) structure, could possibly be the candidate for nucleophilic attack on the acyl intermediate. The phenyl ring of the inhibitor is located at a hydrophobic site which is formed by the sidechains of Leu23, Ile58, Ile70, Met73 (and the corresponding residue in the other subunit, Met573) and Val170 (Figure 3). This hydrophobic site seems to be large enough to accommodate medium chain fatty acids but too small for long chain fatty acids. We suggest that this is the structural basis for the relatively broad specificity toward the acid part of the substrate.

When the enzyme is inhibited by PMSF, no gross structural changes occur (Figure 5). Superimposition of subunit A from the free and inhibitor-bound structures gives rms deviations for 1746 mainchain and 1618 sidechain atoms of 0.23 Å and 0.37 Å, respectively. The largest deviation (0.78 Å) for mainchain atoms is observed for Pro75 in subunit A. The small change associated with inhibitor binding is consistent with the fact that the diffusion of PMSF into the pre-grown crystals caused little deterioration. Cutinase was previously found to be unique among lipolytic enzymes in displaying only small structural changes upon inhibitor binding [19]. In contrast, lipases undergo very large conformational changes from the closed to the open state, in which an inhibitor is covalently bound [30]. This striking difference is largely due to the absence of a flexible lid and also the presence of a preformed oxyanion hole in this carboxylesterase and cutinase. In view of these common structural features, we suggest that cutinase is evolutionarily more closely related to this carboxylesterase than to lipases, even though it shows the lipolytic activity. The observed structural similarity raises the possibility that this carboxylesterase can be modified to enlarge its substrate specificity to allow the hydrolysis of triglycerides of long chain fatty acids.

Subunit interactions

This carboxylesterase exists as a homodimer in solution and monomers are not detected [27]. Active-site clefts of the two subunits face toward each other in a head-to-head fashion in the dimer (Figure 5). Two regions of the carboxylesterase subunit are involved in the dimerization (Figures 5 and 6). The first is the structural region around Tyr167 and His199 (Figure 6a). His199 is one of the catalytic residues and its mainchain nitrogen atom forms a hydrogen bond with the carboxylate oxygen atoms of Asp669 in the other subunit , which is adjacent to the catalytic residue Asp668 (Figure 6a). It is possible that the

Figure 4

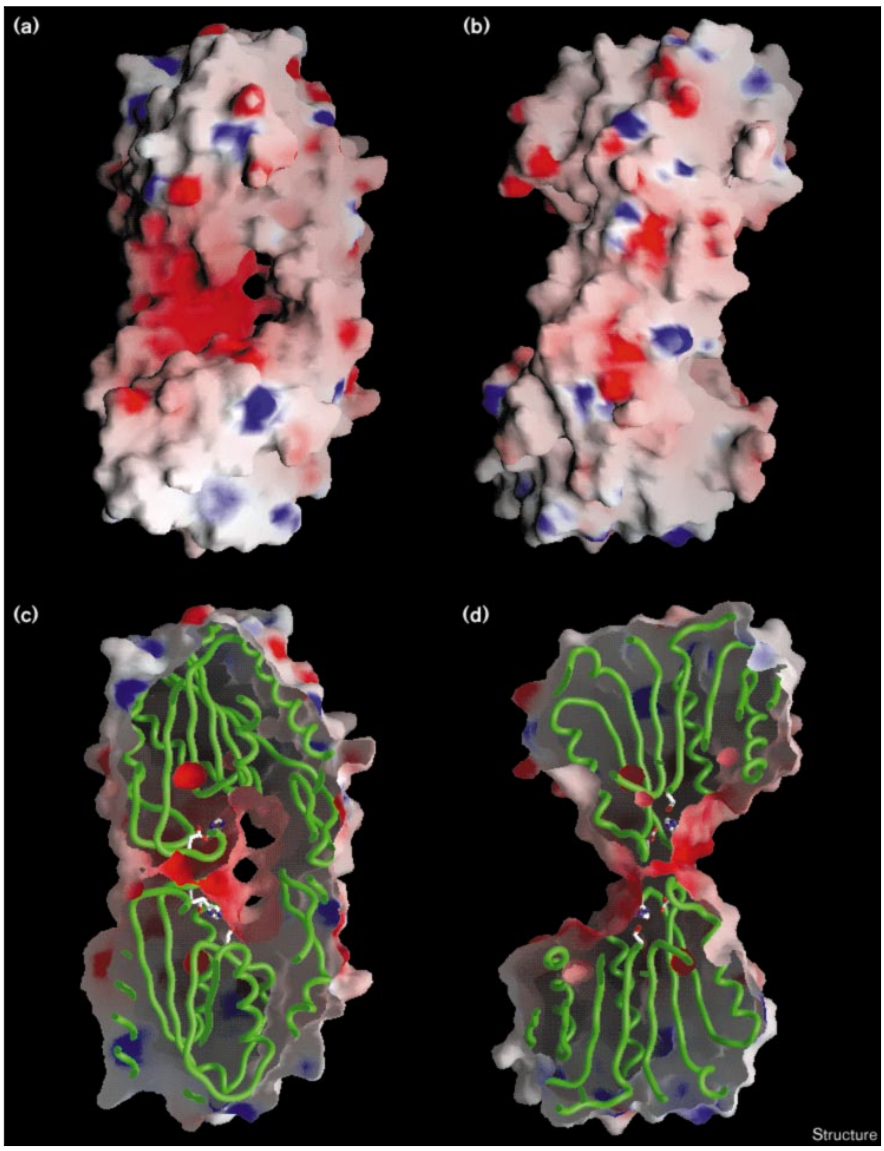

Molecular surface showing the electrostatic potential of carboxylesterase. **(a)** A view showing the holes through the dimer. The non-crystallographic symmetry axis lies horizontally. **(b)** A view obtained by a 90° rotation around a vertical axis. **(c)** The cutaway view of (a). **(d)** The cutaway view of (b). In (c) and (d), the catalytic residues are shown in stick representation and the backbone is shown as green tubes. Negatively charged regions are red and positively charged regions blue. (The figure was drawn with the program GRASP [52].)

breakage of this interaction may have some influence on the catalytic activity. The second dimerization region is the structural region around Ile58 and Met73 (Figure 6b). The latter residue is part of the unique β-hairpin-like structure formed by residues 70–79. Mutations on the above two structural regions may allow dissociation of the two subunits, yielding a monomeric enzyme. In the case of cholesterol esterase, which also exists as a homodimer, the active-site residues are not involved in the intersubunit contact, because the active sites are located far from the dimer interface [24]; therefore, the subunit interaction in the dimer is probably not essential for its catalytic activity. Further studies involving mutagenesis and structure determination are necessary to better understand the possible role of subunit interactions in the catalytic function of this carboxylesterase and to establish if this dimeric carboxylesterase can be redesigned into a functional monomeric enzyme.

The crystal structure of cutinase in complex with an inhibitory triglyceride analogue shows that the two protein molecules in the asymmetric unit are oriented head-to-head, with their substrate-binding sites facing and interacting with each other [19]. This structural arrangement of cutinase allows the large hydrophobic surface, formed by the substrate-binding region itself and by the inhibitor molecule, to be shielded from the solvent. The burying of hydrophobic surfaces in the crystal lattice by means of dimerization has been also observed in other lipase and esterase complexes [24,31], as well as in an open form of

Figure 5

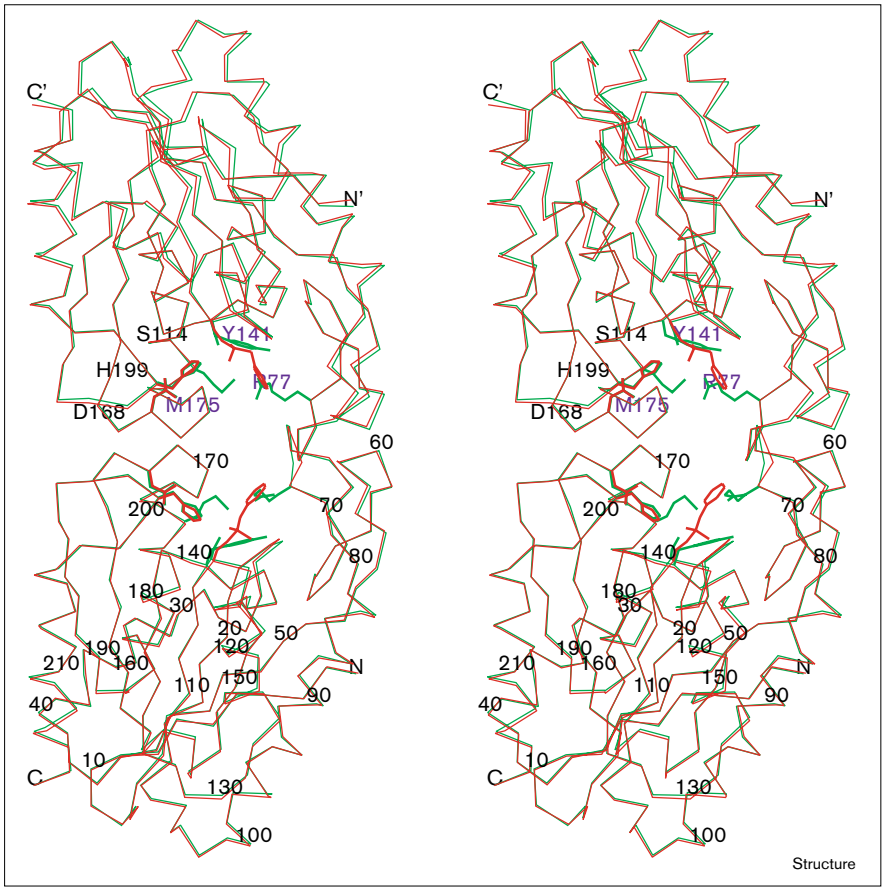

Stereo Cα superposition of the carboxylesterase dimer in the uninhibited (green lines) and inhibited (red lines) states. The non-crystallographic pseudo-twofold axis lies horizontally. Every tenth residue and both the N and C termini are labeled. Three catalytic residues are shown in thicker lines and labeled, along with the covalently bound inhibitor. Sidechains of three residues in each subunit that partially block one side of the active site are drawn in green.

lipase from *Candida rugosa* (CRL; [13]) Cholesterol esterase from *Candida cylindracea* exists as both monomeric and dimeric forms, with dimerization being influenced by the substrate cholesterol linoleate which appears to stabilize the more active dimeric form [32]. In the free structure of cutinase, the extended active-site crevice is partly covered by two thin bridges formed by the sidechain atoms of residues Leu81 and Val184, and Leu182 and Asn84 Cβ [18]. This kind of thin bridge is not fully formed in the subunit structure of carboxylesterase from *P. fluorescens*. Instead, a similar shielding of the hydrophobic substrate-binding site of this carboxylesterase is achieved through dimerization.

Comparisons with other α/β hydrolases and a structural basis for substrate specificity

The 218-residue subunit of *P. fluorescens* carboxylesterase is relatively small by comparison to other α/β hydrolase fold enzymes with known structures. It shows only limited sequence identity with other small α/β hydrolase fold enzymes such as DLH [21] and cutinase [18]. Between carboxylesterase and DLH, about 61 residues can be aligned to be identical (28% identity), whereas between carboxylesterase and cutinase roughly 38 residues are identical (17% identity). DLH with 236 residues has an extra α helix and an extra β strand (Figures 2 and 7a). Cutinase, the smallest known member with 199 residues in the native enzyme, has only five strands in the central β sheet ([18]; Figures 2 and 7b), corresponding to β3–β7 of the prototypic α/β hydrolase fold [8]. In cutinase, the missing last strand (β8), as well as a helix corresponding to αE in carboxylesterase, is replaced by a winding loop of irregular structure between the catalytic residues Asp175 and His188 (Figures 2 and 7b).

Despite the low sequence identity, the catalytic triad and the central β sheet of carboxylesterase subunit superimpose well with those of DLH or cutinase (Figure 7). This is not surprising because these are the best conserved structural features in α/β hydrolase fold enzymes. If 46 Cα atoms of the central β sheet (β2–β8) as well as the catalytic triad in each subunit of carboxylesterase are superimposed with the structurally equivalent atoms of DLH, the rms difference is 1.10 Å for both subunits. A superposition of 36 Cα atoms in the catalytic triad and the central β sheet (β3–β7) of cutinase onto those of carboxylesterase gives a rms difference of 1.05 Å and 1.03 Å, respectively. The central β sheet of

Figure 6

Stereo diagram of subunit–subunit interface in the dimer. Regions **(a)** I and **(b)** II. Subunits A and B are drawn in black and gray, respectively. The residues involved in the subunit interactions are labeled.

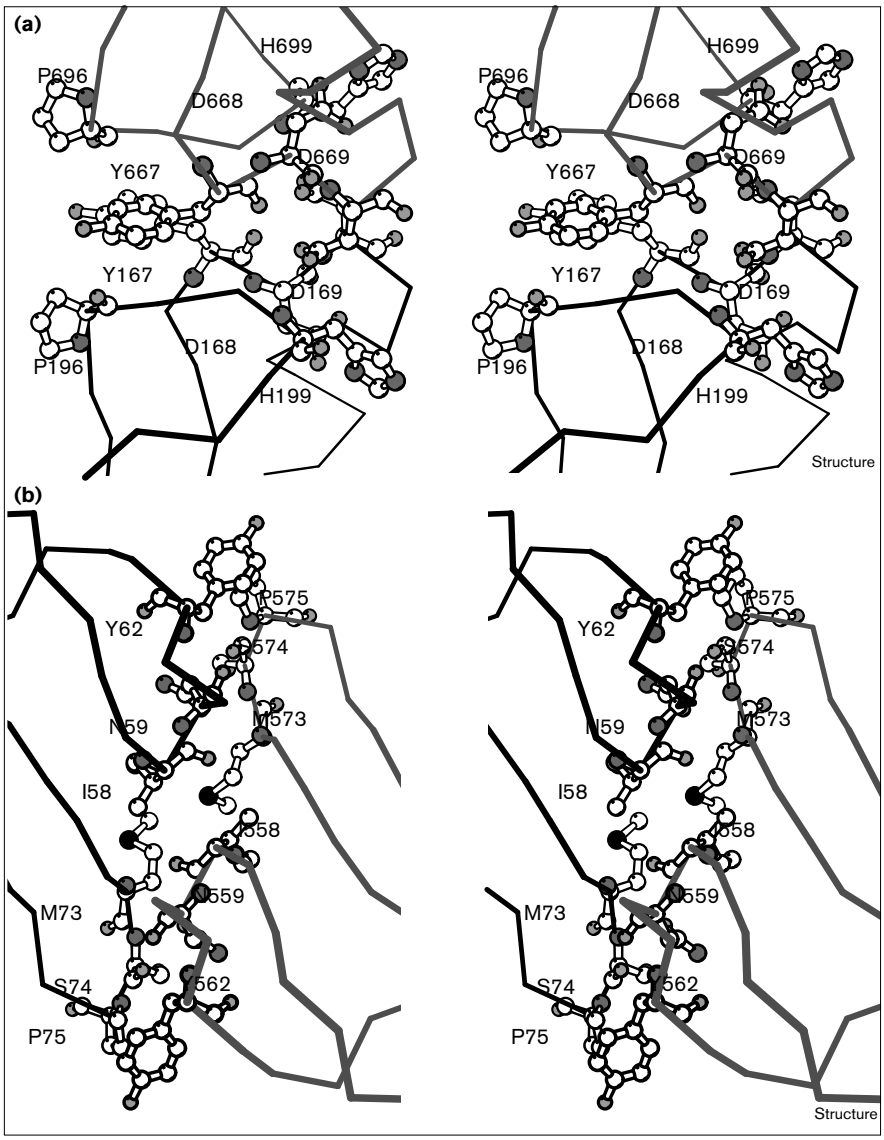

carboxylesterase is slightly more twisted than those of DLH and cutinase. If either the first two or the last two strands are excluded from the comparison, then the superpositions give smaller rms differences. On the other hand, a superposition of the remaining structural elements is not straightforward due to large differences in many parts.

The active-site cleft of carboxylesterase is more open than that of DLH [33], an enzyme with a narrower substrate specificity (Figures 7a and 8). Major differences in the active sites are the presence of an extra loop in DLH (residues 205–217), which contains Arg206, a residue implicated in the substrate binding, and the replacement of one of the active site cleft walls in carboxylesterase (residues 54–80) by a helical segment (residues 65–91) in DLH ([33]; Figure 7a). Cutinase, showing relatively broad substrate specificity, also does not possess a segment corresponding to the inserted loop in DLH (Figures 7b and 8). It is interesting to note that the open sides of the active sites of carboxylesterase and DLH are switched, and the DLH active site is less assessable from the open side of the carboxylesterase active site (Figures 7a and 8).

Both *P. fluorescens* carboxylesterase and cutinase exhibit substrate specificities broad enough to hydrolyze triglycerides as well as carboxylic acid esters [27,34], but the carboxylesterase shows a narrower substrate specificity than cutinase with regard to the length of fatty acids. They share an open active-site cleft (Figures 7b and 8), but the detailed structures around their active-site clefts are

Figure 7

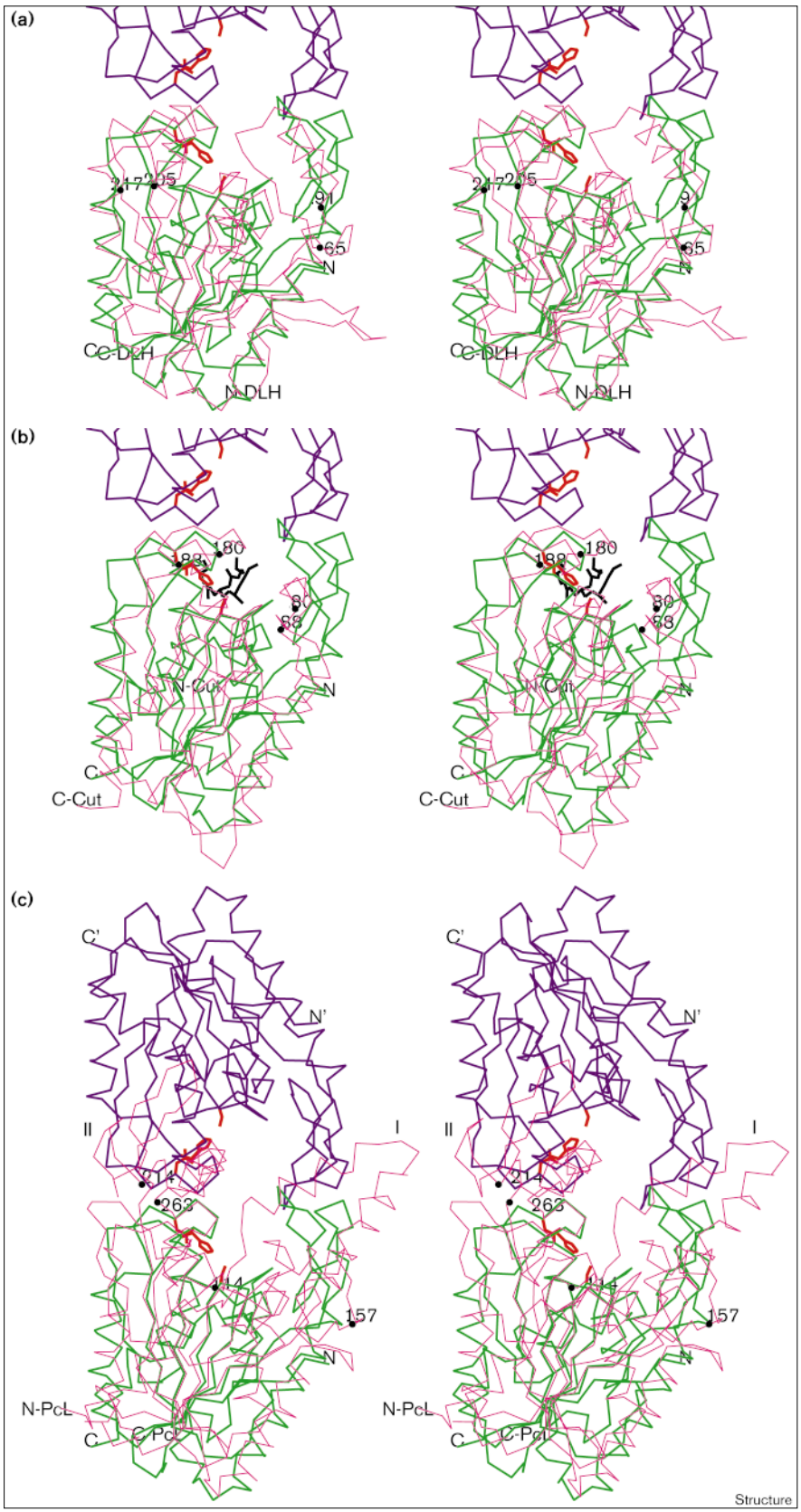

Stereo Cα superposition of *P. fluorescens* carboxylesterase (green lines for subunit A and blue lines for subunit B) and other α/β hydrolases (pink lines). The central β sheet and the catalytic triad of carboxylesterase have been superimposed with those of other hydrolases. The three catalytic residues are colored in red in all parts of the figure. The residues of noteworthy regions of the other hydrolases are indicated by dots and are labeled. **(a)** Comparison with dienelactone hydrolase (DLH). **(b)** Comparison with cutinase (Cut) in complex with a triglyceride analogue (thick black lines for the inhibitor molecule). **(c)** Comparison with *P. cepacia* lipase (PcL) in its open conformation. Two structural regions of PcL that are missing from the carboxylesterase subunit are denoted as regions I (residues 114–157) and II (residues 214–263). In the closed conformation of a highly homologous lipase from *P. glumae*, the region I (lid) covers the active-site cleft.

Figure 8

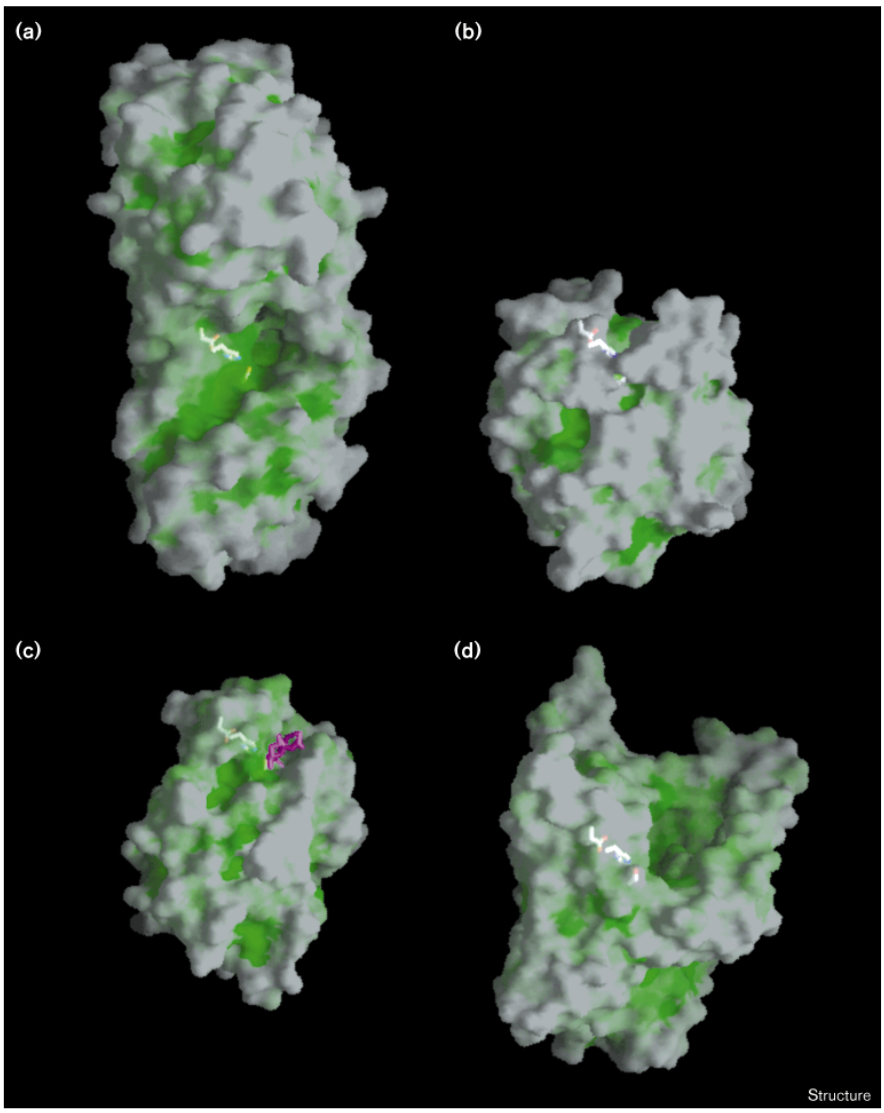

Molecular surface representation illustrating the hydrophobicity. **(a)** *P. fluorescens* carboxylesterase, **(b)** DLH, **(c)** cutinase and **(d)** PcL. The hydrophobic regions are shown in dark green. The catalytic residues, shown in white color through the semi-transparent surface, have the same orientation in these views. In (b) and (d), the catalytic residues are actually behind the front surface. In (c), the bound inhibitor is drawn in magenta. (The figure was drawn with the program GRASP [52].)

different [18–20]. The characteristic loops 80–88 and 180–188 of cutinase which form the thin bridge at the top of the cleft [18] are absent in carboxylesterase (Figure 7b). The crystal structure of cutinase in the covalent complex with the inhibitor (5)-1,2-dibutyl-carbamoylglycero-3-O-*p*-nitrophenylbutyl-phosphonate, a triglyceride analogue, shows that the *sn*-1 and *sn*-2 chains are packed in the lipid-binding site, which is formed by the above characteristic loops and the *sn*-3 chain is accommodated in a rather small pocket at the bottom of the active-site crevice [19]. Cutinase is able to hydrolyze long chain triglycerides (triolein), without any interfacial activation [18,19], although it shows a preference for short chain fatty acid esters. *P. fluorescens* carboxylesterase, however, shows little activity on triacylglycerides of longer than four-carbon fatty acids [27]. This difference may be due to the presence in carboxylesterase of the winding loops encompassing the strands S1, S2, S3 and S4 (Figures 1 and 2) that are absent in cutinase. These extra structural elements in the dimeric structure of carboxylesterase appear to block the binding of long chain fatty acid esters (Figures 7b and 8). It will be interesting to see if this carboxylesterase can be transformed into a cutinase-like lipolytic esterase by removing the above extra segments from its sequence. It seems that the open active-site cleft of this enzyme is one of the contributing factors for the broad substrate specificity. And the extent of the exposure of the active site is probably one of the key elements for determining the substrate specificity of serine esterases. The determinants of substrate specificity, however, are known to correlate not only with structural features of the active site, but also with an inherent capacity for structural deformability of the loops that define the

substrate-binding pocket [35]. For instance, it was difficult to alter the specificity of trypsin due to the high degree of inherent rigidity in structural elements involved in transition-state stabilization, but an analysis of variant α-lytic protease structures suggests that an inherent flexibility of the binding pocket is crucial for the ease of specificity modification [35]. The open active site and a relatively large hydrophobic binding site for the acid part of the substrate revealed in this study thus provide at least a partial explanation for the relatively broad substrate specificity of dimeric carboxylesterase from *P. fluorescens*. Further studies are necessary to understand the structural basis of the substrate specificity of this enzyme in more detail, however.

When the structure of the carboxylesterase subunit is compared with the highly open, active, conformation of PcL [16], two regions of PcL (residues 114–157 and 214–263, labeled as I and II, respectively, in Figure 7c) are absent in carboxylesterase. The active-site cleft in PcL is covered by a cap (region II in Figure 7c); a smaller cap is also present in acetylcholinesterase (AChE; [23]). In the dimeric structure of carboxylesterase, the position of one subunit suggests it to have a possible role as a cap for the other subunit (Figure 7c), although its significance in the catalytic function is unclear. In the active, open, conformation of PcL, the active-site cleft is not covered by an α-helical lid (region I in Figure 7c and Figure 8). But in the inactive, closed, conformation of the highly homologous lipase from *P. glumae*, the catalytic triad is completely buried and is inaccessible to the solvent [12]. The active site of AChE is located at the bottom of a deep gorge, but it is connected to the solvent in both inhibited and uninhibited states [23,36]. This homodimeric carboxylesterase has a relatively open active-site cleft, more open than that in the active, open, conformations of PcL ([16]; Figures 7c and 8) and that in AChE [23]. The catalytic triads in both carboxylesterase subunits are readily accessible to the solvent (Figures 4 and 5). The carboxylesterase differs from PcL in that it does not have a flexible lid and its active-site crevice is shallower than that of PcL. The latter difference is another possible factor responsible for the inability of the carboxylesterase to hydrolyze triglycerides of long chain fatty acids.

In contrast to the presence of many aromatic groups in the substrate-binding sites of CRL and AChE, carboxylesterase has mainly aliphatic sidechains (Figure 3). In AChE, the positive quaternary group of acetylcholine and other cholinergic ligands makes close contacts with aromatic residues [36]. In the case of carboxylesterase, the alcohol part of the substrate probably interacts with a few residues in the loops from the C-terminal ends of β3, β5 and β8 (residues Gly22, Leu23, Phe113 and possibly His199), by analogy with cutinase [19], PcL [16], *Rhizomucor miehei* lipase [37] and AChE [36]. The present crystal structure of *P. fluorescens* carboxylesterase not only provides an indispensable information necessary for protein engineering of this enzyme and other closely-related α/β hydrolases to alter the substrate specificity or the catalytic activity, but it also contributes to a better understanding of an evolutionary relationship among them.

Biological implications

Many man-made chemicals including drugs and pesticides are ester compounds. Their hydrolysis is catalyzed by esterases. One group of esterases, classified as carboxylesterases, catalyze the hydrolysis of short chain aliphatic and aromatic carboxylic ester compounds. Microbial carboxylesterases are useful in stereoselective synthesis of ester compounds and also in stereospecific hydrolysis, due to their broad substrate specificity and high stereoselectivity. In mammals, carboxylesterases play a role in the activation of prodrugs.

In comparison to their close relatives, lipases which like carboxylesterase are α/β hydrolase fold enzymes, structural information on the family of carboxylesterases is very limited. Here, we report the first crystal structure of a member of such a family, carboxylesterase from *Pseudomonas fluorescens*, a homodimeric enzyme of 218-residue subunits. We have determined the structures of both the free enzyme and that of the enzyme in complex with the inhibitor PMSF. Its subunit size is among the smallest of the α/β hydrolase fold enzymes. The subunit structure has the α/β hydrolase fold, but it lacks the first β strand of the prototypic α/β hydrolase fold. The structure allows an unambiguous assignment of the catalytic triad as Ser114–His199–Asp168; it is Ser114 which is covalently modified by inhibitor binding. There is little structural change between the uninhibited and inhibited enzymes. And the oxyanion hole, defined by nitrogen atoms of Leu23 and Gln115, is preformed as in cutinase, a lipolytic enzyme. This contrasts with lipases, in which the oxyanion hole is not formed in the closed inactive state and large conformational changes accompany the transition from the closed to the open state upon inhibitor binding. The catalytic serine residue of carboxylesterase is located at the bottom of the active-site cleft and the inside surface of the surrounding walls is composed of mainly aliphatic sidechains. In the dimer, the active-site clefts from each subunit merge to form holes.

Despite a common catalytic mechanism shared by serine esterases, such as carboxlyesterase, and lipases, they exhibit widely different substrate specificities. *P. fluorescens* carboxylesterase has a relatively broad specificity with regard to the acid part of the substrate, and it is also capable of hydrolyzing triacetin and tributyrin. The large hydrophobic substrate-binding site and an open active site, with the catalytic triad being exposed to the solvent, appear to contribute to the relatively broad substrate specificity of carboxylesterase. This carboxylesterase shows some structural similarity to cutinase, but, in

contrast, it is incapable of hydrolyzing triglycerides of long chain fatty acids. This may be due to the extra structural elements in carboxylesterase that are involved in the head-to-head dimerization. This study reveals not only similarities and dissimilarities between this carboxylesterase structure and those of related enzymes, but it also provides vital structural information for the protein engineering of this enzyme and other closely related α/β hydrolase fold enzymes to alter their substrate specificities. In addition, it also contributes to a better understanding of the evolutionary relationship among members of the α/β hydrolase superfamily.

Materials and methods

Crystallization

Crystallization of the uninhibited enzyme was achieved by the hanging drop vapor diffusion method at room temperature (22 ± 2°C) as described previously [38], under the following reservoir conditions: 0.10 M HEPES buffer at pH 7.76 containing 1.4 M ammonium sulfate, 0.20 M lithium sulfate and 4.0% (v/v) dioxane. The PMSF-inhibited carboxylesterase crystals were prepared by diffusing the inhibitor into the pre-grown crystals as follows. 1 µl of PMSF solution (0.10 M in *n*-propanol) was added to a 10 µl drop containing carboxylesterase crystals. The drop was then sealed again above 1 ml of the reservoir solution and the inhibition reaction was allowed to proceed. An essentially complete inhibition of the enzyme in the crystal was confirmed by observing that no color change takes place upon adding the substrate *p*-nitrophenyl acetate to the crystals in the drop after binding of PMSF to the enzyme. No significant deterioration of the diffraction quality of the crystals resulted from this procedure.

X-ray data collection

For phase determination by multiple isomorphous replacement method, nine heavy-atom derivatives, including two double derivatives and two triple derivatives, were prepared using the crystals of the uninhibited enzyme (Table 1). Data sets from native and heavy-atom derivative crystals were collected on a FAST area detector (Enraf-Nonius) using the MADNES software [39]. CuKα radiation from a Rigaku RU200 rotating X-ray generator, operating at 40 kV and 70 mA, was used with a graphite monochromator. The reflection intensities were obtained by the profile fitting procedure [40] and the data were scaled by the Fourier scaling program [41]. The native crystal belongs to the tetragonal space group $P4_12_12$ or its enantiomorph with unit cell dimensions of a = b = 82.01 Å and c = 145.44 Å, as refined by the MADNES software [39]. The presence of one homodimer in the asymmetric unit gives V_M of 2.56 Å^3/Da and a solvent fraction of 52.0% [38]. The data set of PMSF-inhibited enzyme is 88.5% complete to 2.5 Å. Refined unit cell parameters of a = b = 81.49 Å and c = 144.53 Å were obtained.

Later, synchrotron data from uninhibited crystals were collected at 14°C using a Weissenberg camera for macromolecular crystallography at the BL-6A2 experimental station of Photon Factory, Tsukuba, Japan [42]. The wavelength of X-rays was 1.000 Å and a 0.1 mm collimator was used. A Fuji image plate (type BAIII, 20 × 40 cm) was placed at a distance of 429.7 mm from the crystal. The oscillation range per image plate was 5.0° with a speed of 2.0°/s and a coupling constant of 1.0°/mm for the a-axis rotation, and it was 4.5° with a speed of 2.0°/s and a coupling constant of 1.8°/mm for the c-axis rotation. An overlap of 0.5° was allowed between two contiguous image plates. The diffraction patterns recorded on the image plates were digitized by a Fuji BA100 scanner. The raw data were processed using the program WEIS [43]. The data of the uninhibited enzyme consisted of 262,303 measurements of 41,703 unique reflections with an R_{merge} (on intensity) of 7.1% (rejecting 4.5% outliers). The merged data set is 90.1% complete to 1.8 Å. Refined unit cell parameters of a = b = 82.04 Å and c = 145.38 Å were obtained.

Structure determination

Three-dimensional difference Patterson maps were calculated with 12.0–4.0 Å data and heavy atoms were located using the program HASSP [44] in the CCP4 package [45]. Minor heavy-atom sites were located in the cross-phase difference Fourier maps. The three derivatives (Pt, Hg1 and Hg3 in Table 1) share a common heavy-atom site; the two derivatives Hg1 and Hg2 share three sites; and the derivatives Hg3 and Hg4 share two sites. Heavy-atom parameters were refined by the program MLPHARE in the CCP4 package [45]. The anomalous difference data allowed the assignment of the correct space group as $P4_12_12$. In the final cycle of phase determination, the mean figure of merit was 0.76 for 12.0–3.2 Å data. The non-crystallographic symmetry (NCS) axis was determined from the heavy-atom sites. The statistics for the heavy-atom refinement are given in Table 1.

The electron density corresponding to seven β strands and several α helices in one subunit in the asymmetric unit was clear, whereas that in the other subunit was less clear. The initial model of a subunit was built in 25 fragments with 167 residues. Using the molecular envelope defined by this partial model, phases were improved and extended to 2.6 Å by the program SQUASH through NCS averaging, solvent flattening, Sayer equation and histogram matching [46]. The electron-density map calculated with SQUASH phases was more readily interpretable than the MIR map and all 218 residues in one subunit could be unambiguously assigned. The other subunit was generated by using the NCS relationship and some manual model adjustment.

Model refinement

Crystallographic refinement was carried out using the X-PLOR program package [47]. Initially, data in the 8.0–3.0 Å range were used in the refinement, and the high resolution limit was extended in steps to 1.8 Å. The NCS between the two independent subunits in the asymmetric unit was maintained with tight restraint during the early stage of the refinement, but it was relaxed in the final rounds of refinement. After simulated annealing by the standard slow cooling protocol starting from 3000 K to 300 K, 100 cycles of energy minimization were followed. Isotropic B factors were initially set to 15.0 Å^2 and refined in the last stages of the refinement with restraint. Extensive model rebuilding was carried out between each stage. Solvent molecules were placed by searching the model-phased (F_o–F_c) maps.

The crystallographic refinement of PMSF-inhibited carboxylesterase was also carried out using the X-PLOR program package [47]. The rigid-body refinement using low resolution data was performed using the refined model of uninhibited carboxylesterase, followed by the conventional energy minimization and simulated annealing with 8.0–2.5 Å data. R_{free} was monitored during the refinement using 10% of total reflections as a test data set. Model-phased (F_o–F_c) maps were used to model the bound inhibitors. A modified residue Sep114 was made by covalently linking PMSF with Ser114. The sulfur atom of the inhibitor is covalently bound to the oxygen atom Oγ of Ser114. Successive refinement was continued using the 8.0–2.5 Å data. Other procedures regarding the refinement of B factors and inclusion of water molecules are essentially the same as for the uninhibited case.

Model building and structure analysis

Model building was performed with the graphics program FRODO [48], running on an Evans and Sutherland PS390 graphics system, and with CHAIN version 7.2 [49], running on a Silicon Graphics Indigo^2 XZ workstation. At each stage of the model rebuilding and refinement, the stereochemistry of the model was assessed by the program PROCHECK [50]. The secondary structure elements were assigned by the program PROMOTIF [51]. Structural comparisons were made using the program LSQKAB in CCP4 program package [45].

Accession numbers

The atomic coordinates and structure factor data are available from the Protein Data Bank with accession codes 1auo (uninhibited) and 1aur (inhibited) for atomic coordinates; r1auosf (uninhibited) and r1aursf (inhibited) for structure factor data.

Acknowledgements

We thank David Ollis and Christian Cambillau for kindly providing the coordinates of dienelactone hydrolase and cutinase. We also thank N Sakabe, A Nakagawa, and N Watanabe for assistance during data collection at BL-6A2 of the Photon Factory, Japan. The X-ray equipment provided by the Inter-University Center for Natural Science Research Facilities was supported in part by the Korea Science Engineering Foundation Specialization Fund. We gratefully acknowledge financial support from the Korea Ministry of Education (International Cooperative Research Program), the Korea Science and Engineering Foundation through the Center for Molecular Catalysis at Seoul National University, and the Basic Science Research Institute, MOE (97-3418).

References

1. Krish, K. (1971). Carboxylic ester hydrolysis. In *The Enzymes*. (Boyer, P.D., ed), Vol. 5, pp. 43–69, Academic Press, New York.
2. Gaustad, R., Sletten, K., Lovhaug, D. & Fonnum, F. (1991). Purification and characterization of carboxylesterase from rat lung. *Biochem. J.* **274**, 693–697.
3. Tombo, G.M.R., Schar, H.-P. & Ghisalba, O. (1987). Application of microbes and microbial esterases to preparation of optically active N-acetylindoline-2-carboxylic acid. *Agric. Biol. Chem.* **51**, 1833–1838.
4. Toone, E.J., Werth, M.J. & Jones, J.B. (1990). Active-site model for interpreting and predicting the specificity of pig liver esterase. *J. Am. Chem. Soc.* **112**, 4946–4952.
5. Sobek, H. & Grisch, H. (1989). Further kinetic and molecular characterization of an extremely heat-stable carboxylesterase from thermoacidophilic archaebacterium *Sulfolobus acidocaldarius*. *Biochem. J.* **261,** 993–998.
6. Rathbone, D.A., Holt, P.-J., Lowe, C.R. & Bruce, N.C. (1996). The use of a novel recombinant heroin esterase in the development of an illicit drugs biosensor. *Ann. N.Y. Acad. Sci.* **799**, 90–96.
7. Rivory, L.P., Bowles, M.R., Robert, J. & Pond, S.M. (1996). Conversion of irinotecan (CPT-11) to its active metabolite, 7-ethyl-10-hydroxycamptothecin (Sn-38), by human liver carboxylesterase. *Biochem. Pharmacol.* **52**, 1103–1111.
8. Ollis, D.L. *et al.*, & Goldman, A. (1992). The α/β hydrolase fold. *Protein Eng.* **5**, 197–211.
9. Brady, L., *et al.*, & Brozozowski, A.M. (1990). A serine protease triad forms the catalytic centre of a triacylglycerol lipase. *Nature* **343**, 767–770.
10. Winkler, F.K., D'Arcy, A. & Hunziker, W. (1990). Structure of human pancreatic lipase. *Nature* **343**, 771–774.
11. Schrag, J.D. & Cygler, M. (1993). 1.8 Å refined structure of the lipase from *Geotrichum candidum*. *J. Mol. Biol.* **230**, 575–591.
12. Noble, M.E.M., Cleasby, A., Johnson, L.N., Egmond, M.R. & Frenken, L.G.J. (1993). The crystal structure of triacylglycerol lipase from *Pseudomonas glumae* reveals a partially redundant catalytic aspartate. *FEBS Lett.* **331**, 123–128.
13. Grochulski, P., *et al.*, & Cygler, M. (1993). Insights into interfacial activation from an open structure of *Candida rugosa* lipase. *J. Biol. Chem.* **268**, 12843–12847.
14. Derewenda, U., *et al.*, & Derewenda, Z.S. (1994). An unusual buried polar cluster in a family of fungal lipases. *Nat. Struct. Biol.* **1**, 36–47.
15. Uppenberg, J., Hansen, M.T., Patkar, S. & Jones, T.A. (1994). The sequence, crystal structure determination and refinement of two crystal forms of lipase B from *Candida antarctia*. *Structure* **2**, 293–308.
16. Kim, K.K., Song, H.K., Shin, D.H., Hwang, K.Y. & Suh, S.W. (1997). The crystal structure of a triacylglycerol lipase from *Pseudomonas cepacia* reveals a highly open conformation in the absence of a bound inhibitor. *Structure* **5**, 173–185.
17. Schrag, J.D., *et al.*, & McPherson, A. (1997). The open conformation of a *Pseudomonas* lipase. *Structure* **5**, 187–202.
18. Martinez, C., De Geus, P., Lauwereys, M., Matthyssens, G. & Cambillau, C. (1992). *Fusarium solani* cutinase is a lipolytic enzyme with a catalytic serine accessible to solvent. *Nature* **356**, 615–618.
19. Longhi, S., *et al.*, & Cambillau, C. (1997). Crystal structure of cutinase covalently inhibited by a triglyceride analogue. *Protein Sci.* **6**, 275–286.
20. Longhi, S., Czjzek, M., Lamzin, V., Nicolas, A. & Cambillau, C. (1997). Atomic resolution (1.0 Å) crystal structure of *Fusarium solani* cutinase: stereochemical analysis. *J. Mol. Biol.* **268**, 779–799.
21. Pathak, D. & Ollis, D. (1990). Refined structure of dienelactone hydrolase at 1.8 Å. *J. Mol. Biol.* **214**, 497–525.
22. Verschueren, K.H.G., Franken, S.M., Rozeboom, H.J., Kalk, K.H. & Dijkstra, B.W. (1993). Refined X-ay structures of haloalkane dehalogenase at pH 6.2 and pH 8.2 and implications for the reaction mechanism. *J. Mol. Biol.* **232**, 856–872.
23. Sussman, J.L., *et al.*, & Harel, M. (1991). Atomic structure of acetylcholinesterase from *Torpedo californica*: a prototypic acetylcholine-binding protein. *Science* **253**, 872–879.
24. Ghosh, D., *et al.*, & Duax, W. (1995). Structure of uncomplexed and linoleate-bound *Candida cylindracea* cholesterol esterase. *Structure* **3**, 279–288.
25. Liao, D.-I., Breddam, K., Sweet, R.M., Bullock, T. & Remington, S.J. (1992). Refined atomic model of wheat serine carboxypeptidase II at 2.2 Å resolution. *Biochemistry* **31**, 9796–9812.
26. Lawson, D.M., *et al.*, & Derewenda, Z.S. (1994). Structure of a myristoyl-ACP-specific thioesterase from *Vibrio harveyi*. *Biochemistry* **33**, 9382–9388.
27. Hong, K.H., Jang, W.H., Choi, K.D. & Yoo, O.J. (1991). Characterization of *Pseudomonas fluorescens* carboxylesterase: cloning and expression of the esterase gene in *Escherichia coli*.. *Agric. Biol. Chem.* **55**, 2839–2845.
28. Brenner, S. (1988). The molecular evolution of genes and proteins: a tale of two serines. *Nature* **334**, 528–530.
29. Martinez, C., *et al.*, & Cambillau, C. (1994). Cutinase, a lipolytic enzyme with a preformed oxyanion hole. *Biochemistry* **33**, 83–89.
30. Derewenda, Z.S. (1994). Structure and function of lipases. *Adv. Protein Chem.* **45**, 1–52.
31. van Tilbeurgh, H., Egloff, M.-P., Martinez, C., Rugani, N., Verger, R. & Cambillau, C. (1993). Interfacial activation of the lipase–procolipase complex by mixed micelles revealed by X-ray crystallography. *Nature* **362**, 814–820.
32. Kaiser, R., Erman, M., Duax, W.L., Ghosh, D. & Jörnvall, H. (1994). Monomeric and dimeric forms of cholesterol esterase from *Candida cylindracea*. *FEBS Lett.* **337**, 123–127.
33. Cheah, E., Ashley, G.W., Gary, J. & Ollis, D. (1993). Catalysis by dienlactone hydrolase: a variation on the protease mechanism. *Proteins* **16**, 64–78.
34. Lauwereys, M., de Geus, P., de Meutter, J., Stanssens, P. & Matthyssens, G. (1991). Cloning, expression, and characterization of cutinase – a lipolytic enzyme. In *Lipases: Structure, mechanism and genetic engineering*. (Alberghina, L., Schmid, R.D. & Verger, R., eds), pp. 416–452, VCH, Weinheim.
35. Tsu, C.A., Perona, J.J., Fletterick, R.J. & Craik, C.S. (1997). Structural basis for the broad substrate specificity of fiddler crab collagenolytic serine protease 1. *Biochemistry* 36, 5393–5401.
36. Harel, M., *et al.*, & Sussman, J.L. (1993). Quaternary ligand binding to aromatic residues in the active-site gorge of acetylcholinesterase. *Proc. Natl. Acad. Sci. USA* **90**, 9031–9035.
37. Brozozowski, A.M., *et al.*, & Derewenda, U. (1991). A model for interfacial activation in lipase from the structure of a fungal lipase–inhibitor complex. *Nature* **351**, 491–494.
38. Kim, K.K., *et al.*, & Suh, S.W. (1993). Crystallization and preliminary X-ray crystallographic analysis of carboxylesterase from *Pseudomonas fluorescens*. *Arch. Biochem. Biophys.* **302**, 417–419.
39. Messerschmidt, A. & Pflugrath, J.W. (1987). Crystal orientation and X-ray pattern prediction routines for area-detector diffractometer systems in macromolecular crystallography. *J. Appl. Cryst.* **20**, 306–315.
40. Kabsch, W. (1988). Evaluation of single-crystal X-ray diffraction data from a position-sensitive detector. *J. Appl. Cryst.* **21**, 916–924.
41. Weissman, L. (1982). Strategies for extracting isomorphous and anomalous signals. In *Computational Crystallography*. (Sayre, D., ed.), pp. 56–63, Oxford University Press, Claredon.
42. Sakabe, N. (1993). X-ray diffraction data collection system for modern protein crystallography with a Weissenberg camera and an imaging plate using synchrotron radiation. *Nucl. Instrum. Methods A* **303**, 448–463.
43. Higashi, T. (1989). The processing of diffraction data taken on a screenless Weissenberg camera for macromolecular crystallography. *J. Appl. Cryst.* **22**, 9–18.
44. Terwilliger, T.C., Kim, S.-H. & Eisenberg, D. (1987). Generalized method of determining heavy-atom positions using the difference patterson function. *Acta Cryst. A* **43**, 1–5.
45. CCP4 (1994). Collaborative Computational Project Number 4. The CCP4 suite: programs for protein crystallography. *Acta Cryst. D* **50**, 760–763.
46. Zhang, K.Y.J. (1993). SQUASH: combining constraints for macromolecular phase refinement and extension. *Acta Cryst. D* **49**, 213–222.
47. Brünger, A.T., Kuriyan, J. & Karplus, M. (1987). Crystallographic R-factor refinement by molecular dynamics. *Science* **235**, 458–460.
48. Jones, T.A. (1985). Interactive computer graphics: FRODO. *Methods Enzymol.* **115**, 157–171.
49. Sack, J.S. (1988). CHAIN: a crystallographic modelling program. *J. Mol. Graphics* **6**, 244–245.
50. Laskowski, R.A., MacArthur, M.W., Moss, D.S. & Thornton, J.M. (1993). PROCHECK: a program to check the stereochemical quality of protein structures. *J. Appl. Cryst.* **26**, 283–291.
51. Hutchinson, E. & Thornton, J.M. (1996). PROMOTIF: a program to identify and analyze structural motifs in proteins. *Protein Sci.* **5**, 212–220.
52. Nicholls, A., Sharp, K.A. & Honig, B. (1991). Protein folding and association: insights from the interfacial and thermodynamic properties of hydrocarbons. *Proteins* **11**, 281–293.